FLUTTER CHARACTERISTICS OF TYPICAL WING SECTIONS OF A BOX WING AIRCRAFT CONFIGURATION

S. Ahmad Fazelzadeh [(1)], Dieter Scholz [(2)], Abbas Mazidi [(3)], Michael I. Friswell[(4)]

[(1)] Shiraz University, School of Mechanical Engineering, Molla-Sadra Street, 71963-16548, Shiraz, Iran, Email: Fazelzad@shirazu.ac.ir
[(2)] Hamburg University of Applied Sciences, Aircraft Design and Systems Group (AERO), Berliner Tor 9, 20099 Hamburg, Germany, Email: info@ProfScholz.de
[(3)] Yazd University, Faculty of Mechanical Engineering, Safaeih, Yazd, Iran, Email: amazidi@yazd.ac.ir
[(4)] Swansea University, College of Engineering, Swansea University Bay Campus, Swansea SA1 8EN, United Kingdom, Email: m.i.friswell@swansea.ac.uk

KEYWORDS: Flutter, BWA, Typical Section Model, Green Aviation, Box Wing

ABSTRACT:

In this paper, the aeroelastic modeling and conceptual flutter analysis of a simple 2-D box wing is investigated. For each wing the torsion and bending elasticity is simulated by two torsional and longitudinal springs at its elastic axis. Furthermore, the connection winglet is simulated by a longitudinal spring. The aeroelastic governing equations are derived using Lagrange's equations. Also, for aeroelastic loads simulation on the box wing, the Theodorsen aerodynamic model is used. The effects of various design parameters such as front and rear wing physical and geometrical properties, the connection winglet angle and stiffness, and aircraft altitude on the flutter of the system are investigated. Results show that the connection winglet stiffness and angle have significant influence on the box wing flutter boundary.

1. INTRODUCTION

The interaction between wing structural dynamics and aerodynamic loading is referred to as wing dynamic aeroelasticity. There are many dynamic phenomena in aeroelasticity, but the most important dynamic instability is flutter. Wing flutter is a dynamic instability of a wing associated with the interaction of aerodynamic, elastic, and inertial forces, which generally leads to a catastrophic structural failure of the wing [1]. Because of the catastrophic nature of flutter, it is important that it is identified and avoided in the design phase. Indeed, the flight envelope is typically limited by the speed at which flutter occurs.
Much of the immediate interest in abatement strategies focuses on rapid commercialization of green aviation technologies. Research into green aviation technology including reduced noise, emissions and fuel consumption has grown fast in recent years. In order to meet these goals, several new technology ideas and innovative aircraft configurations are being investigated by airplane designers. Innovative configurations combine the main parts of an aircraft (wing, fuselage, tail ...) in an un-conventional way with the intention to save on fuel burn and emissions. One such configuration is the Box Wing Aircraft (BWA).
The BWA belongs to the nonplanar lifting system category of airplane configurations. It is a biplane which has a fuselage which is similar to conventional aircraft. Its lifting system consists of two wings, where the front one is swept-back and the rear one is swept-forward. The tips of both wings are connected by a vertical winglet. Figure 1 shows the box wing aircraft model developed by AERO at Hamburg University of Applied Sciences. The most recognized benefit of this configuration is its low induced drag.

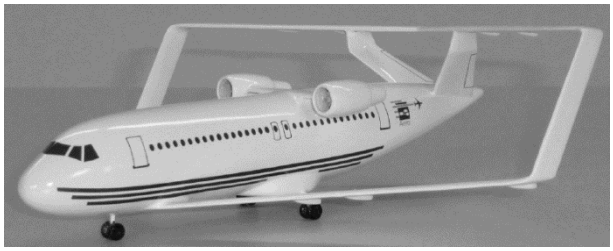

Figure 1. A typical box wing aircraft [2].

Figure 1 shows only one possible BWA configuration. Many others have been proposed [3]. The evaluation of flutter clearance for such new concept wings is a major aeronautical engineering task. Clearly estimating the aeroelastic instabilities is critical to establishing the flight envelope of newly designed aircraft. The first recorded and documented case of flutter in an aircraft occurred in 1916 [4]. After that, during the First World War, catastrophic failures due to aircraft flutter became a major design concern. The first study of the flutter of aircraft wings was compiled by Frazer and

Duncan in 1928. They introduced methods for analysis and prevention of flutter that are the basis for techniques in use today. In recent decades, because of the increase in wing flexibility and speeds, flutter analysis has become one of the most important aspects of wing design and, consequently, a lot of research has been done in this field. Although, the large quantity of papers associated with wing flutter analysis makes it almost impossible to consider them all, flutter researches on clean wings [5, 6], wings carrying external stores [7-9], wings with powered engines [10, 11], maneuvering wings [12, 13], and morphing wing models [14, 15] gives an idea of the range of research done in this area.

Different studies on BWA designs have been presented in previous research. Initial investigations were implemented by Prandtl who introduced the box wing aircraft as the best wing system [16]. Subsequently some theoretical investigations have been performed by researchers. More recent studies have focused on the design of different commercial aircraft with the box wing configuration [17-21]. In most of this research some design aspects, such as aeroelastic constraints, were not considered in the design procedure. Figure 2 shows, for example, the recommendations plot for further improvement of the box wing design which was presented by Zohlandt [22]. He presented the conceptual design of a high subsonic box wing aircraft and performed three comparison studies between box wing aircraft and conventional aircraft and showed that the box wing configuration has great potential. In Fig. 2, each item has been ranked on a scale from 1 to 5 on its level of complexity and also the level of urgency to implement this improvement to the design. The resulting matrix shows the high necessity of aeroelastic considerations in box wing aircrafts design.

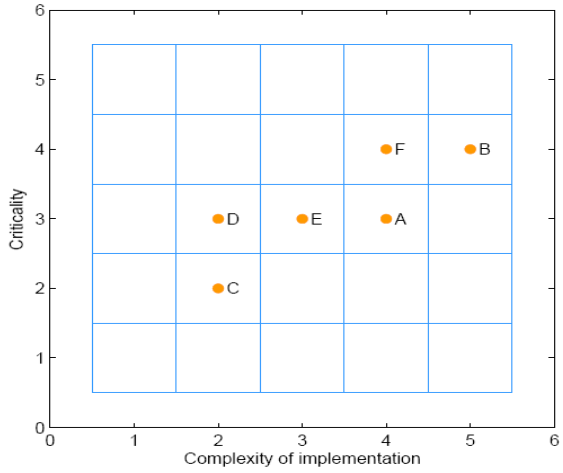

A Double Deck Aircraft
B Aeroelastic Behaviour
C Landing Gear Nacelles
D Landing Gear weight Estimation Improvement
E EMWET Connector Weight
F Automated BoxWing Sizing and Positioning

Figure 2. Recommendations plot showing urgency vs. complexity of the implementations needed for improvement of the box wing design [22].

In recent years some works have been initiated to study the BWA aeroelasticity [23-26], although there is not yet a wide literature studying the aeroelasticity of Box Wings and several aspects need to be understood and analyzed in more depth. In this study, the aeroelastic modeling and flutter analysis of a BWA configuration is investigated. The results of this study can help designers to introduce small modifications to the design or come up with new BWA configurations that would avoid the flutter problem.

2. AEROELASTIC MODELING

In this research the aeroelastic conceptual analysis of a simple 2-D box wing as shown in Fig.3 is considered. In Fig. 3(a) the box wing aircraft is illustrated. The typical wing tip section is represented in Fig. 3(b), where h_F and θ_F denote the plunge and pitch motion of the front wing and h_A and θ_A denote the plunge and pitch motion of the aft wing. Wing and wingtip are considered to be connected with a ball joint giving no restriction to any relative rotational motion.

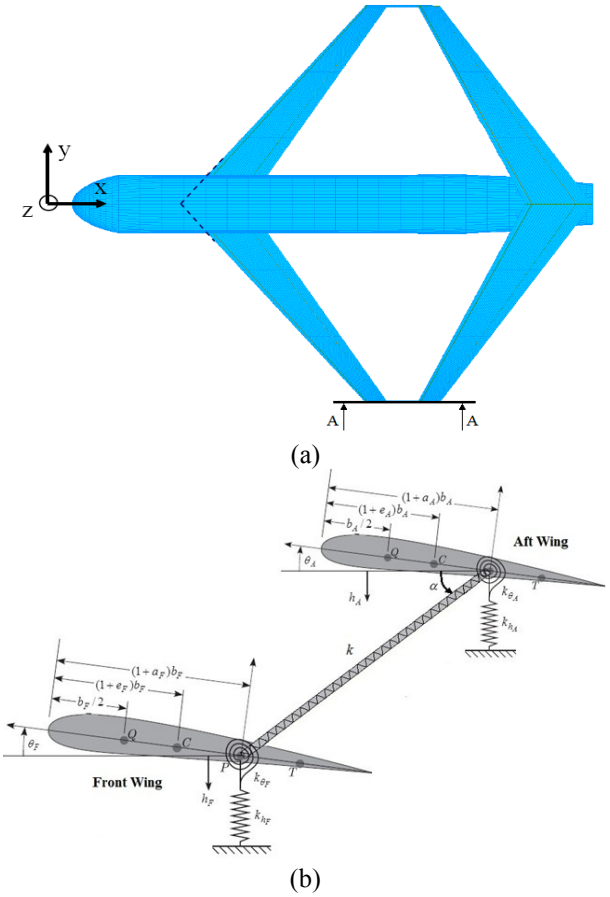

Figure 3. (a) Schematic of a box wing aircraft (b) Section A-A of the box wing.

The aeroelastic governing equations are derived using Lagrange's Equations:

$$\frac{d}{dt}\left(\frac{\partial T}{\partial \dot{q}_i}\right)+\frac{\partial P}{\partial q_i}=Q_i \qquad (1)$$

where P and T are the strain energy and the kinetic energy, and Q_i is the generalized force. Also, the q_i are generalized coordinates which are defined as:

$$\mathbf{q} = \{h_F \;\; \theta_F \; h_A \;\; \theta_A\} \tag{2}$$

The total kinetic energy of the box wing is simply:

$$T = T_F + T_A \tag{3}$$

where T_F and T_A are the front and aft wing kinetic energies, respectively, which are:

$$T_F = \frac{1}{2} m_F \left(\dot{h}_F{}^2 + 2 b_F x_{\theta F} \dot{h}_F \dot{\theta}_F \right) + \frac{1}{2} I_{PF} \dot{\theta}_F{}^2 \tag{4}$$

$$T_A = \frac{1}{2} m_A \left(\dot{h}_A{}^2 + 2 b_A x_{\theta A} \dot{h}_A \dot{\theta}_A \right) + \frac{1}{2} I_{PA} \dot{\theta}_A{}^2 \tag{5}$$

The strain energy is given by:

$$\begin{aligned} P = {} & \frac{1}{2} k_{hF} h_F{}^2 + \frac{1}{2} k_{\theta F} \theta_F{}^2 + \frac{1}{2} k_{hA} h_A{}^2 + \\ & \frac{1}{2} k_{\theta A} \theta_A{}^2 + \frac{1}{2} k (h_F - h_A)^2 \sin^2(\alpha) \end{aligned} \tag{6}$$

Furthermore, the virtual work of non-conservative forces acting on the wing may be expressed as:

$$\begin{aligned} \delta W = {} & L_F \left[-\delta h_F + b_F \left(\frac{1}{2} + a_F \right) \delta\theta_F \right] + M_F \delta\theta_F + \\ & L_A \left[-\delta h_A + b_A \left(\frac{1}{2} + a_A \right) \delta\theta_A \right] + M_A \delta\theta_A \end{aligned} \tag{7}$$

which leads to the following generalized forces:

$$\begin{aligned} Q_{hF} &= -L_F \\ Q_{\theta F} &= M_F + b_F \left(\frac{1}{2} + a_F \right) L_F \\ Q_{hA} &= -L_A \\ Q_{\theta A} &= M_A + b_A \left(\frac{1}{2} + a_A \right) L_A \end{aligned} \tag{8}$$

Substituting Eqs. (3)-(8) into Eq. (1) the aeroelastic governing equations are obtained as:

$$\begin{aligned} & m_F \left(\ddot{h}_F + b_F x_{\theta F} \ddot{\theta}_F \right) + k_{hF} h_F + \\ & k (h_F - h_A) \sin^2(\alpha) = -L_F \\ & I_{pF} \ddot{\theta}_F + m_F b_F x_{\theta F} \ddot{h}_F + \\ & k_{\theta F} \theta_F = M_F + b_F \left(\frac{1}{2} + a_F \right) L_F \\ & m_A \left(\ddot{h}_A + b_A x_{\theta A} \ddot{\theta}_A \right) + k_{hA} h_A - \\ & k (h_F - h_A) \sin^2(\alpha) = -L_A \\ & I_{pA} \ddot{\theta}_A + m_A b_A x_{\theta A} \ddot{h}_A + \\ & k_{\theta A} \theta_A = M_A + b_A \left(\frac{1}{2} + a_A \right) L_A \end{aligned} \tag{9}$$

The aerodynamic forces are derived from the Theodorsen quasi-steady aerodynamic model. Using this model, the aerodynamic lift and moment for the front wing and the aft wing can be written as:

$$\begin{aligned} L_F = {} & C_{LF} \rho_\infty U b_F \left[\dot{h}_F + U\theta_F + b_F \left(\frac{1}{2} - a_F \right) \dot{\theta}_F \right] \\ & + \frac{1}{2} C_{LF} \rho_\infty b_F{}^2 \left(\ddot{h}_F + U\dot{\theta}_F - b_F a_F \ddot{\theta}_F \right), \\ M_F = {} & -\frac{1}{2} C_{LF} \rho_\infty b_F{}^3 \\ & \left[\frac{1}{2} \ddot{h}_F + U\dot{\theta}_F + b_F \left(\frac{1}{8} - \frac{a_F}{2} \right) \ddot{\theta}_F \right] \\ L_A = {} & C_{LA} \rho_\infty U b_A \left[\dot{h}_A + U\theta_A + b_A \left(\frac{1}{2} - a_A \right) \dot{\theta}_A \right] \\ & + \frac{1}{2} C_{LA} \rho_\infty b_A{}^2 \left(\ddot{h}_A + U\dot{\theta}_A - b_A a_A \ddot{\theta}_A \right), \\ M_A = {} & -\frac{1}{2} C_{LA} \rho_\infty b_A{}^3 \\ & \left[\frac{1}{2} \ddot{h}_A + U\dot{\theta}_A + b_A \left(\frac{1}{8} - \frac{a_A}{2} \right) \ddot{\theta}_A \right] \end{aligned} \tag{10}$$

Substituting Eq. (10) into Eq. (9) the following set of ordinary differential equations are obtained.

$$\mathbf{M}\ddot{\mathbf{q}} + \mathbf{C}\dot{\mathbf{q}} + \mathbf{K}\mathbf{q} = \mathbf{0} \tag{11}$$

Herein, **M**, **C** and **K** denote the mass matrix, the damping matrix and the stiffness matrix, respectively, while **q** is the overall vector of generalized coordinates.

3. RESULTS AND DISCUSSION

Following the *p* method, states of the box wing aeroelastic system are considered as:

$$\begin{aligned} h_F &= \bar{h}_F \exp(vt) \\ \theta_F &= \bar{\theta}_F \exp(vt)) \\ h_A &= \bar{h}_A \exp(vt) \\ \theta_A &= \bar{\theta}_A \exp(vt)) \end{aligned} \tag{12}$$

Substituting Eq. (12) into Eq. (11) the following set of algebraic equations are obtained:

$$\left[\mathbf{M}\lambda^2 + \mathbf{C}\lambda + \mathbf{K} \right] \mathbf{q} = \mathbf{0} \tag{13}$$

For a nontrivial solution to exist, the determinant of the coefficient matrix must be set equal to zero. The λ's are continuous functions of the air speed U. For $U \neq 0$, λ is in general complex, and hence $\lambda = \mathrm{Re}(\lambda) + i\,\mathrm{Im}(\lambda)$. When $\mathrm{Re}(\lambda) = 0$ and $\mathrm{Im}(\lambda) \neq 0$ the wing is said to be in the critical flutter condition. At some point, as U increases, $\mathrm{Re}(\lambda)$ turns from negative to positive so that the motion turns from asymptotically stable to unstable.

Pertinent data for the particular wing used here are considered in Table 1. Also, the dimensionless parameter used in the numerical simulation is:

$$K = k / k^* \tag{14}$$

where $k^* = EA / l'$, and EA and l' are the winglet tension stiffness and length, respectively.

In Fig. 4, the modal damping of the box wing is

plotted versus the air speed. The connection winglet has an angle of $\alpha = 45$ deg and its stiffness is $K = 0.5$. The flutter condition is marked by the crossing of the real part of one of the roots into positive zone. The flutter speed obtained is $v_f = 81\text{m/s}$, and there is modal damping in all of the modes below the flutter speed.

Table 1. Characteristics of the Box Wing Model

Parameters	Value
l	6.1 m
l'	2 m
b_F	0.915 m
m_F	35.695 kg/m
I_{PF}	7.172 kg·m
a_F	-0.2
e_F	-0.1
k_{hF}	$1.29 \cdot 10^5$ N/m
$k_{\theta F}$	$1.62 \cdot 10^5$ N/m
b_A	0.732 m
m_A	28.56 kg/m
I_{PA}	3.672 kg·m
a_A	-0.2
e_A	-0.1
k_{hA}	$1.03 \cdot 10^5$ N/m
$k_{\theta A}$	$1.3 \cdot 10^5$ N/m
EA	$6.56 \cdot 10^5$ N
ρ_∞	1.224 kg/m^3
C_{LF}	2π
C_{LA}	2π

The flutter condition is marked by the crossing of the real part of one of the roots into positive zone. The flutter speed obtained is $v_f = 81\text{m/s}$. It can be seen that there is modal damping in all of the modes below the flutter speed.

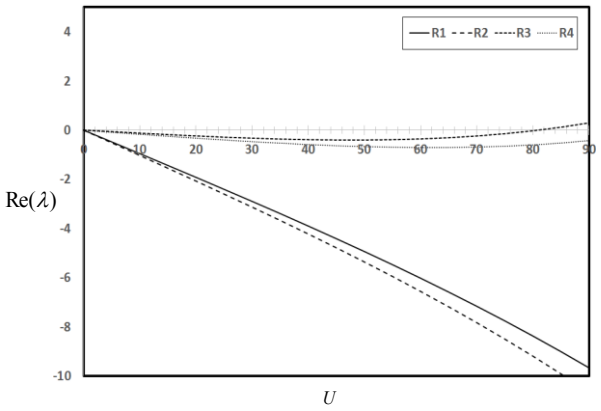

Figure 4. Plot of the modal damping versus the air speed.

Figure 5 shows the variation of the flutter speed and frequency of the box wing for selected values of the connection winglet stiffness due to variations in the front and rear wing bending stiffness. The connection winglet has an angle of $\alpha = 45$ deg. It can be seen from this figure that both flutter speed and frequency significantly increase by increasing the wing bending stiffness. Furthermore, decreasing the connection winglet stiffness improve the stability domain of the wing.

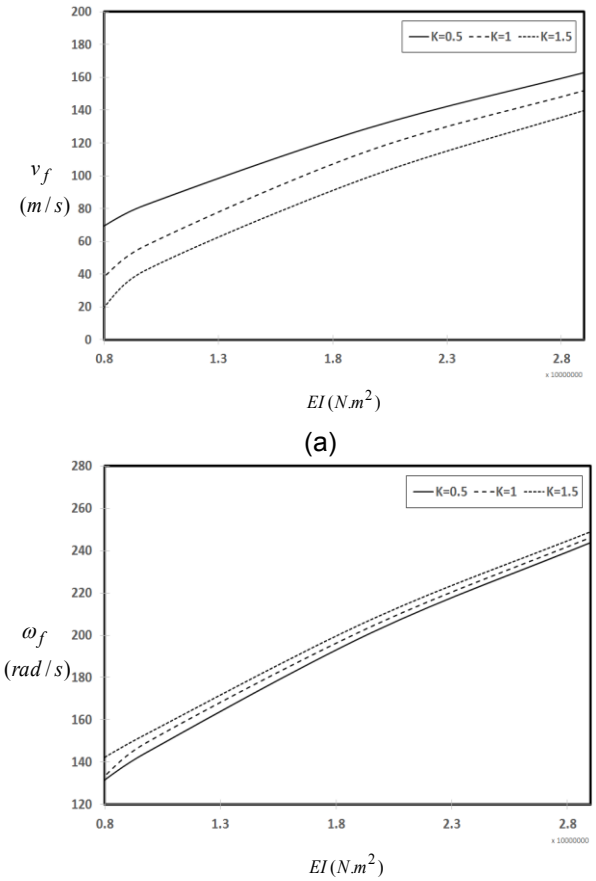

Figure 5. Effects of the wing bending rigidity on the flutter boundary for selected values of the winglet stiffness, (a) Flutter speed, (b) Flutter frequencies.

Figure 6 demonstrates the effect of the connection winglet angle on the box wing flutter boundary at different altitudes. The connection winglet stiffness is $K = 0.5$.

It can be seen that increasing the winglet angle will decrease the flutter speed in all altitudes. This means that increasing the winglet angle decreases the stability domain of the airplane. Furthermore, the effect of the aircraft altitude on the wing flutter speed and frequency is clearly highlighted. The results show an increase of the flutter speed and frequency with increased altitude.

The effects of the wing length on the flutter speed and frequency are shown in Fig. 7. The connection winglet has an angle of $\alpha = 45$ deg and it is assumed that both the front and rear wings have the same length *l*.

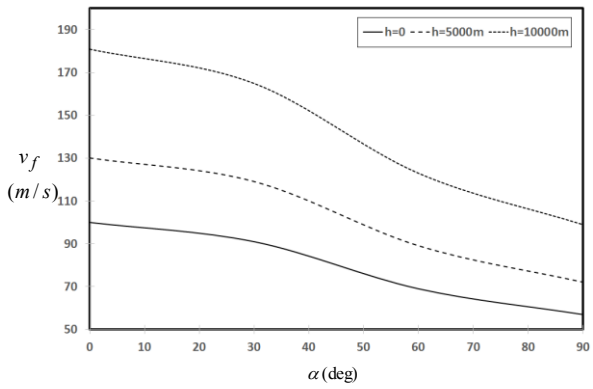

(a)

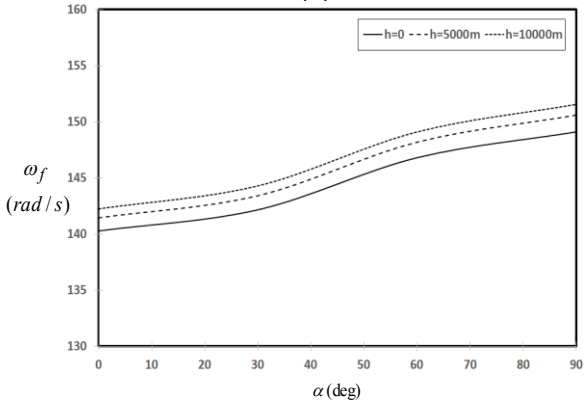

(b)

Figure 6. Effects of the connection winglet angle on the flutter boundary for selected values of the aircraft altitude, (a) Flutter speed, (b) Flutter frequencies.

As expected, by increasing the box wing length the flutter speed and frequency decrease. Both plunge and pitch effective stiffness coefficients reduce by increasing the wing length.

Figure 8 reveals the effect of front to rear wing length ratio on the flutter speed and frequency of the box wing. The connection winglet stiffness is $K=0.5$. The front and rear wing roots are considered fixed and the wing tips move parallel to the aircraft body towards the nose and tail of the body. The length ratio parameter is defined as:

$$L=l_F/l_A \qquad (15)$$

where l_F is the front wing length and l_A is the aft wing length. Figure 8(a) shows that the length ratio has only a small effect on the box wing flutter speed. Only for high values of the connection winglet angle, the lower length ratios expands the flutter stability region of the box wing. Figure 8(b) shows that the front to rear wing length ratio influences the flutter frequency more.

The effect of the wing chord on the flutter speed and frequency is shown in Fig. 9. The connection winglet stiffness is $K=0.5$.

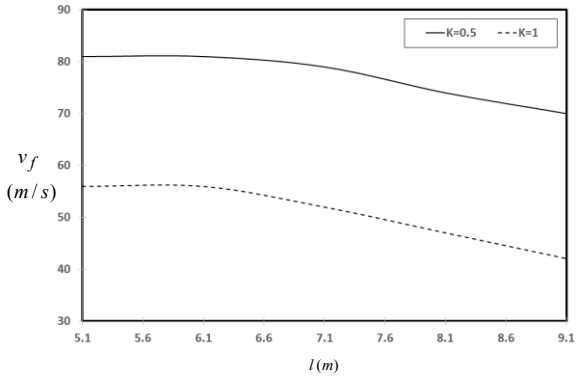

(a)

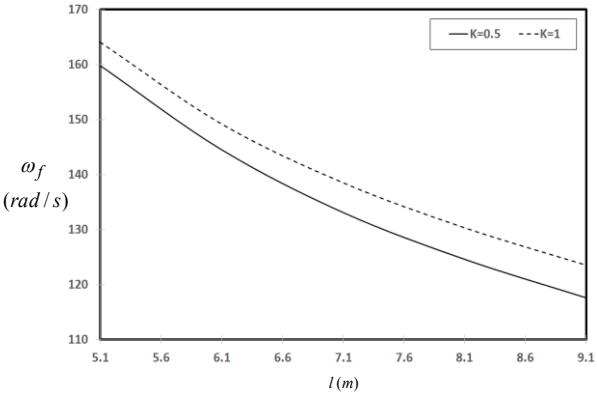

(b)

Figure 7. Effects of the wing length on the flutter boundary for selected values of the winglet stiffness, (a) Flutter speed, (b) Flutter frequencies.

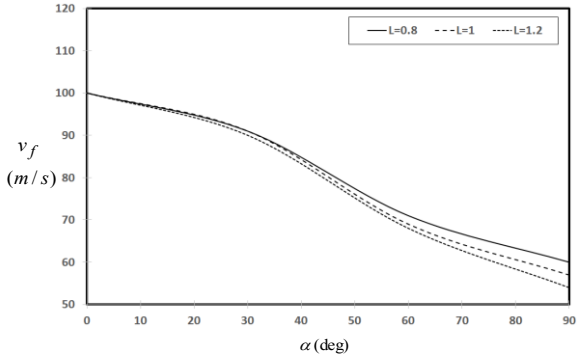

(a)

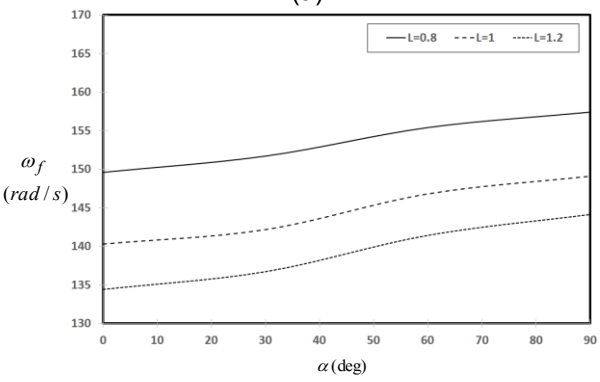

(b)

Figure 8. Effects of the connection winglet angle on the flutter boundary for selected values of the front wing to rear wing length ratios, (a) Flutter speed, (b) Flutter frequencies.

The chord ratio parameter *B* is defined as:

$$B = b / b_{ref} \tag{16}$$

where b is the wing chord and b_{ref} is the reference wing chord given in Table 1. Figure 9(a) shows that the wing chord only has a small effect on the box wing flutter speed. Also, Fig. 9(b) demonstrates that the flutter frequency increases by decreasing the wing chord.

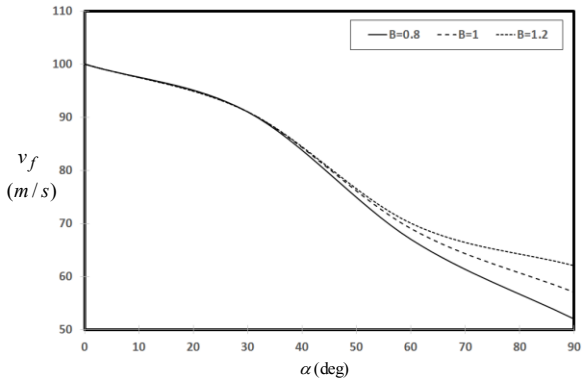

(a)

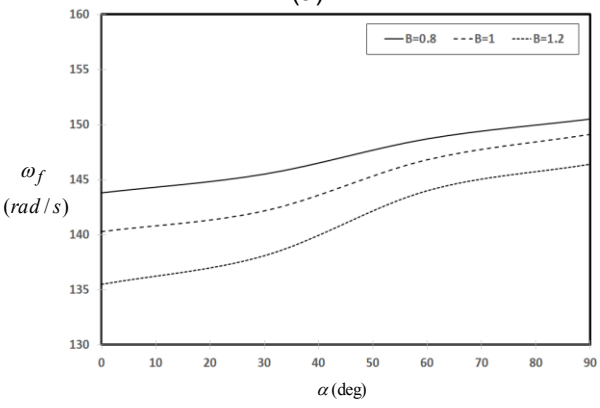

(b)

Figure 9. Effects of the connection winglet angle on the flutter boundary for selected values of the wing chord, (a) Flutter speed, (b) Flutter frequencies.

4. CONCLUSION

Aeroelastic modeling and flutter analysis of a simple 2-D box wing is considered in this study. Plunge and pitch motions of both the rear and front wings are considered in the aeroelastic model. The connection winglet is also modeled as a longitudinal spring.

The effects of various design parameters such as the front and rear wings length, chord, and bending stiffness, and also the connection winglet angle and stiffness, on the box wing flutter are investigated. The results show that increasing the connection winglet stiffness decreases the flutter speed of the box wing. Also, it is observed that flutter speed reduces by increasing the connection winglet angle.

5. RECOMMENDATIONS

The 2-D approach applied here is a first step to the flutter analysis of the BWA. More meaningful results would need a 3-D approach and would need to use several models considering joints with different degrees of freedom between wing and winglet. According to Jemitola [27] the rigid joint provides the lightest structural box wing mass, although the rigid joint itself may be heavier than a ball joint. Schedl et al. [28] found the opposite: They obtained the lightest box wing applying a universal joint with unconstrained x- and z-rotation. The second lightest box wing was obtained applying a ball joint (as considered in this paper).

6. REFERENCES

1. Wright, J.R. & Cooper, J.E. (2007). Introduction to Aircraft Aeroelasticity and Loads, *Wiley*.
2. Scholz, D. (2016). Evolutionary Aircraft Configurations – Possible A320 Successor. Research Project 2008-2014. – URL: http://Airport2030.ProfScholz.de.
3. Barua, P. & Scholz, D. (2013). Systematic Approach to Analyze, Evaluate and Select Box Wing Aircraft Configurations from Modified Morphological Matrices. Technical Note, Aircraft Design and Systems Group (AERO), HAW Hamburg. – URL: https://bit.ly/2MM2tLI
4. Hodges, D.H. & Pierce, G.A. (2011). Introduction to Structural Dynamics and Aeroelasticity, *Cambridge University Press*, Cambridge, UK.
5. Barmby, J.G., Cunningham, H.J. & Garrick, I.E. (1950). Study of Effects of Sweep on the Flutter of Cantilever Wings. NACA TN2121.
6. Haddadpour, H., Kouchakzadeh, M.A. & Shadmehri, F. (2008). Aeroelastic Instability of Aircraft Composite Wings in an Incompressible Flow. *Compos Struct.* **83**, 93–99.
7. Goland, M. & Luke, Y.L. (1948). The Flutter of a Uniform Wing with Tip Weights. *J. Applied Mech*. **15**, 13-20.
8. Librescu, L. & Song, O. (2008). Dynamics of Composite Aircraft Wings Carrying External Stores. *AIAA J*. **46**, 568-572.
9. Fazelzadeh, S.A., Mazidi, A. & Kalantari, H. (2009). Bending-Torsional Flutter of Wings With an Attached Mass Subjected To a Follower Force. *J. Sound Vib*. **323** 148–162.
10. Hodges, D.H., Patil, M.J. & Chae, S. (2002). Effect of Thrust on Bending-Torsion Flutter of Wings. *J. Aircraft*. **39**, 371-376.

11. Mazidi, A. & Fazelzadeh, S.A. (2013). Aeroelastic Modeling and Flutter Prediction of Swept Wings Carrying Twin-Powered-Engines, *J. Aerospace Eng*. **26**, 586–593.

12. Meirovitch, L. & Tuzcu, I. (2003). Integrated Approach to the Dynamics and Control of Maneuvering Flexible Aircraft, *NASA Technical Report*. NASA/CR-2003-211748.

13. Mazidi, A., Fazelzadeh, S.A. & Marzocca, P. (2011). Flutter of Aircraft Wings Carrying a Powered Engine Under Roll Maneuver. J. Aircraft. **48** 874-884.

14. Ajaj, R.M. & Friswell, M.I. (2018). Aeroelasticity of Compliant Span Morphing Wings, *Smart Mat Struct*. Accepted.

15. Wang, C., Khodaparast, H.H., Friswell, M.I., Shaw, A.D., Xia, Y. & Walters, P. (2018) Development of a Morphing Wingtip Based on Compliant Structures. *J. Intelligent Mat Sys Struct*. Accepted.

16. Prandtl, L. (1924). Induced Drag of Multiplanes. NACA Technical Report No. 182.

17. Frediani, A. Gasperini, M. Saporito, G. & Rimondi, A. (2003) Development of a Prandtl Plane Aircraft Configuration. In XVII Congresso Nazionale AIDAA III, Roma, Italy.

18. Frediani, A. & Montanari, G. (2009). Best Wing System: an Exact Solution of the Prandtl's Problem. In Variational Analysis and Aerospace Engineering.

19. Frediani, A., Cipolla, V. & Rizzo, E. (2012). The Prandtl Plane Configuration: Overview on Possible Applications to Civil Aviation. In Variational Analysis and Aerospace Engineering: Mathematical Challenges for Aerospace Design.

20. Schiktanz, D. & Scholz, D. (2011). Box Wing Fundamentals – An Aircraft Design Perspective. In DGLR: Deutscher Luft- und Raumfahrtkongress. – Download from: http://Airport2030.ProfScholz.de.

21. Schiktanz, D. & Scholz, D. (2011). The Conflict of Aerodynamic Efficiency and Static Longitudinal Stability of Box Wing Aircraft. In 3rd CEAS Air & Space Conference - 21st AIDAA Congress. – Download from: http://Airport2030.ProfScholz.de.

22. Zohlandt, C.N. (2016). Conceptual Design of High Subsonic Prandtl Planes-Analysis and Performance Comparison with Conventional Configurations in the High Subsonic Transport Category. Master Thesis, Delft University.

23. Bombardieri R., Cavallaro R. & Demasi L. (2016). A historical Perspective on the Aeroelasticity of Box Wings and Prandtl-Plane with New Findings. In 57th AIAA/ ASCE/ AHS/ ASC Structures, Structural Dynamics, and Materials Conference, San Diego, USA.

24. Silvani, S. (2015). Aeroelastic Analysis of Prandtl Plane Joined Wings Configuration. Master's thesis, Universit`a degli Studi di Roma.

25. Cavallaro, R., Bombardieri, R., Demasi, L. & Iannelli, A. (2015). PrandtlPlane Joined Wing: Body Freedom Flutter, Limit Cycle Oscillation and Freeplay Studies. *J. Fluids Struct*. **59**, 57–84.

26. Cavallaro, R., Bombardieri, R., Silvani, S., Demasi, L. & Bernardini, G. (2016). Aeroelasticity of the PrandtlPlane: Body Freedom Flutter, Freeplay and Limit Cycle Oscillation. In Variational Analysis and Aerospace Engineering: Mathematical Challenges for Aerospace Design.

27. Jemitola, P.O., Fielding, P. & Stocking, P. (2012). Joint fixity effect on structural design of a box wing aircraft, *The Aeronautical Journal*, **116**, 363-372. – DOI: https://doi.org/10.1017/S0001924000005261

28. Schedl, A., Schirra, J. C., Boblenz, A., Bauschat, J.-M. & Spohr, A. (2014). Parametric Study of Structural Weight Estimation for Highly Non-planar Lifting Systems. In DGLR: Deutscher Luft- und Raumfahrtkongress.

This paper was presended by S. Ahmad Fazelzadeh during the conference "Advanced Aircraft Efficient Global Air Transport System" (AEGATS 2018), Toulouse, France, 23.-25.10.2018, organized by the Association Aéronautique et Astronautique de France (3AF) and is part of the AEGATS Proceedings (2018). https://AEGATS2018.com

https://doi.org/10.15488/4097

https://nbn-resolving.org/urn:nbn:de:gbv:18302-aero2018-10-23.019